THE O'DAY AND BIRKELAND IMPACT CRATERS AS PROBES INTO THE INTERIOR OF THE SOUTH POLE-AITKEN BASIN. B. Shankar[1,2] and G. R. Osinski[1,2]. [1]Dept. of Earth Sci, University of Western Ontario, 1151 Richmond St. N., London, ON, Canada. (bshanka@uwo.ca); [2] Canadian Lunar Research Network

Introduction: Several craters within the South Pole-Aitken (SPA) basin have been identified as landing sites of interest, addressing key questions concerning the bombardment history of planetary bodies, differentiation of planetary interiors, and the effects of impact cratering [1, 2]. Recent discoveries of pure anorthosite, Mg-Spinel, and olivine-rich assemblages from orbital data has further fueled the interest to better understand the SPA basin forming process, and about the lunar interior in general [3–5].

The Birkeland and O'Day craters (Fig. 1) are two such craters that have the potential of sampling both highland crust and mafic rich deposits within the SPA basin [2]. Previous studies have noted broad spectral diversities at these sites [6, 7]. Using a combination of spatial, spectral, and topographic datasets, we assess the distribution of impactite materials and determine compositional information about the target subsurface.

Geological setting of the study sites*:* Birkeland and O'Day craters are well preserved complex impact craters located along the north-west quadrant of the SPA basin (Fig. 1A).

Birkeland crater is an Eratosthenian aged complex crater located ~30°S/172°E (Fig. 1B). With a 82 km diameter, it has a well defined crater rim, terraced walls, and a flat crater floor. The central uplift is a consolidated peak with partial slumping along the north-east section. It shares part of the northern crater wall with the double crater Van de Graaff [8]. Several post-Birkeland event craters are located both on the crater floor and beyond the crater rim. Previous studies have noted a strong thorium anomaly near Birkeland [9, 10].

O'Day crater (Fig. 1C), Copernican in age, is located north-west of Mare Ingenii (30.5°S/157.5°E) and has a rim diameter of 71 km. The terraced wall is wider and more pronounced along the western half of the crater. The northern section of the crater floor is flat and filled with smooth materials. The southern section, in contrast, has a mixture of both smooth and rough deposits. The central uplift appears to be partially collapsed.

Methods: Proximal impact materials have been mapped (Fig. 2) using LRO-WAC global mosaics and individual NAC images. Impact melt deposits are identified primarily based on their visible characteristics – smooth deposits that show obvious contrast when compared to their immediate surroundings, and that lack a volcanic source of origin.

Further characterization of the impactite units is accomplished by fusing spectral and spatial data. RGB composite maps are generated from the Chandrayaan-1 Moon Mineralogy Mapper (M^3) UV-VIS-NIR data, comparing the integrated band depth (IBD) parameters at 1µm, 2 µm, and reflectance at 1.58 µm to assess the mineralogy (Fig. 3). IBD values are calculated using algorithms from [11]. Sample spectral profiles are derived using the 85-band M^3 data. Each of the geological units identified in Fig. 2 are sampled to determine preliminary compositional detail of both craters.

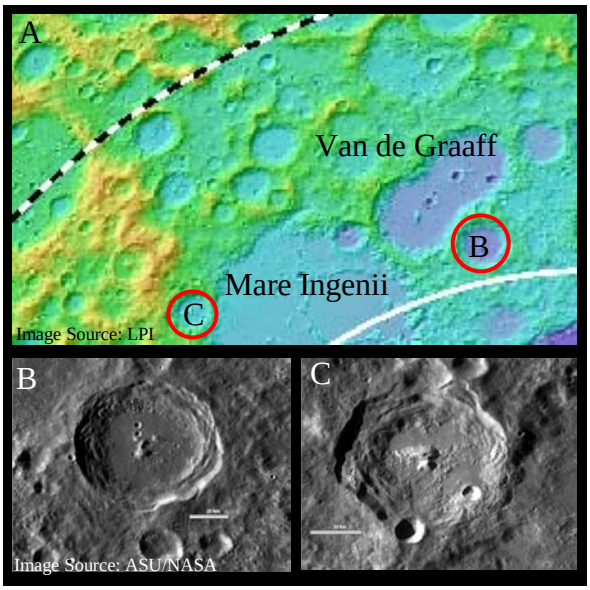

Figure 1: (A) Global LRO-LOLA topography mosaic of the north-west quadrant of the SPA basin. Study sites outlined in red circles. SPA basin extent (black and white dash line) and transient crater diameter (solid white line) are also outlined. (B) LROC-WAC global mosaic view of the 82 km Birkeland crater. Scale bar is 25 km. (C) LROC-WAC global mosaic view of the 71 km O'Day crater. Scale bar is 25 km.

Results: The extent of crater materials are highlighted in the geological sketch maps (Fig. 2). For both craters, the crater floor is filled with large extents of smooth terrain (interpreted as impact melt rich deposits) and some hummocky terrain. Melt deposits are also observed along the terrace walls and overlying impact ejecta.

Spectral data indicate local concentrations of both iron rich (Fig. 3, black arrows) and iron poor (Fig. 3, white arrows) materials. Sampled spectral profiles (Fig. 4) of the morphological units indicate the presence of

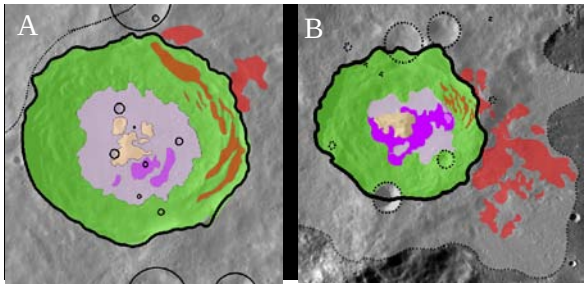

Figure 2: Geologic sketch maps highlight impactite units of (A) Birkeland crater, and (B) O'Day crater. Basemap is LRO wide angle camera (WAC) global mosaics. Grey = crater ejecta; green = terrace walls; light purple = smooth crater floor; dark purple = rough hummocky terrain; pale yellow = central uplift; red = impact melt deposits; bold black line = rim outline; black circles = post impact crater outlines

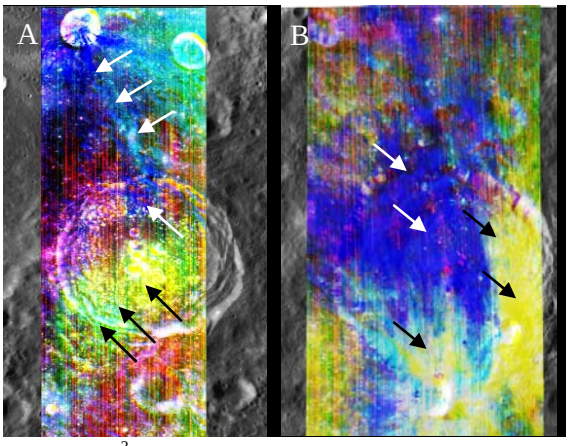

Figure 3: M^3 derived integrated band depth (IBD) parameter RGB composite map of (A) Birkeland crater, and (B) O'Day crater. Red = 1µm IBD; green = 2 µm IBD; blue = reflectance at 1.58 µm.

mostly noritic and gabbroic rock types based on classfication by [12]. The non-ubiquitous distribution of all materials suggest a number of factors control the diverse spread of observed compositions, including pre-existing topography and regional setting.

Discussion: The variable nature of mafic rich content within both Birkeland and O'Day is likely due the presence of similarly mafic rich units in the target subsurface. Iron-poor compositions within the central uplifts suggest the O'Day event probably excavated highland crust. However, the proximity of O'Day crater to Mare Ingenii could explain the concentration of mafic assemblages to the east and south crater walls (Fig. 3B, 4B).

At Birkeland crater, Lunar Prospector data has recorded anomalous thorium concentrations [10], with Th levels higher than within rest of the SPA basin. Multiple hypotheses exist for the source of the elevated Th levels, including the excavation of Th-rich upper crust

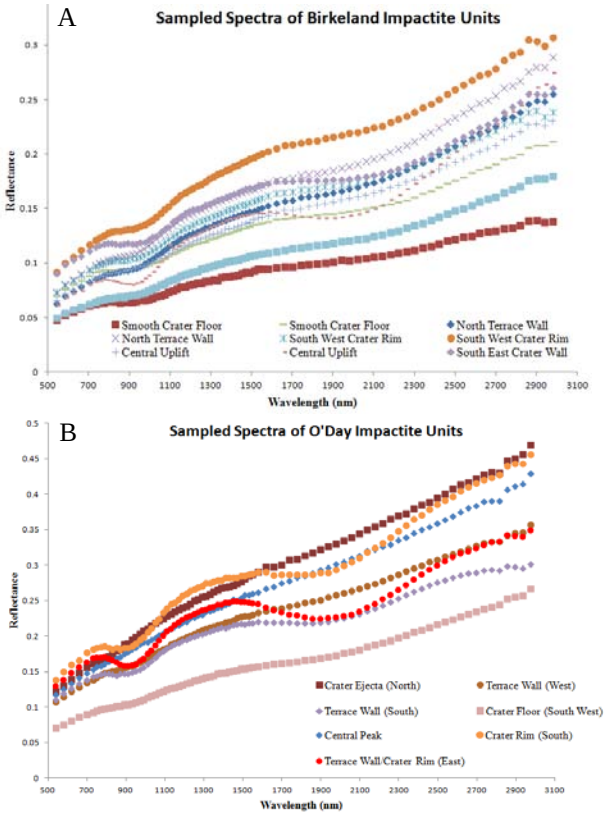

Figure 4: (A) Sample M^3 spectra of Birkeland impactite units. (B) Sample M^3 spectra of O'Day impactite units.

within the SPA [10], a cryptomafic source [13], or within the antipode area of the Imbrium basin [14]. Elevated levels of high Ca-pyroxene to the south west (Fig. 3A) may correlate with Th-anomaly distribution in [10] but this needs further investigation. Both craters are located beyond the transient crater diameter of the SPA (Fig. 1A), therefore the excavated materials could be part of the SPA impact melt sheet or crustal rocks. Ongoing work continues to address these questions.

References: [1] NRC (2007) *The Scientific Context for the Exploration of the Moon*. Washington D.C.: The National Academies Press. 107. [2] *Eds.* D. Kring and D.D. Durda. (2011) *A Global Lunar Landing Site Study to Provide the Scientific Context for Exploration of the Moon*. LPI Contrib. No. 1694, 477–562. [3] Ohtake, M. et al. (2009) *Nature*, 461, 236–240. [4] Yamamoto, S. et al. (2010) *Nature GeoSci.* 3, 8, 533–536. [5] Pieters, C.M. et al. (2011) *JGR*, 116, E6, E00G08 [6] Tompkins, S. and Pieters, C.M. (1999) *MAPS*, *34*, 25–41. [7] Cahill, J.T.S. et al. (2009) *JGR*, 114. E09001. [8] Stuart-Alexander, D.E. (1978) *U.S.G.S. Misc. Inves. Ser. Map* I-1047. [9] Blewett, D. et al. (2000) *LPSC XXXI*, Abstract #1501. [10] Wieczorek, M. and Zuber, M. (2001) *JGR, 106*, 27853–27864. [11] Mustard, J.F. et al. (2011) JGR, 116, E00G12. [12] Pieters, C.M. et al. (2001) *JGR*, 106, E11, 28001– 28022. [13] Hawke, B.R. and Spudis, P. (1980). *Proc. Conf lunar high. crust*, 467–481. [14] Haskin, L.A. (1998) *JGR*, 103, 1679–1689.